Electrochemical performance of a nanostructured $Pd_{70}Co_{20}Mo_{10}$ MEA

Mauricio Garza-Castañón*, M.A. Jiménez, J.L. Acevedo-Dávila
Corporación Mexicana de Investigación en Materiales S.A. de C.V.
Ciencia y Tecnología # 790, Fracc. Saltillo 400, C.P. 25290, Saltillo Coahuila, México

F. Loyola, U. Cano
Hydrogen and fuel cells group, Instituto de Investigaciones Eléctricas, Cuernavaca Morelos
Reforma # 113 Col Palmira, C.P. 62490, Cuernavaca Morelos, México

O.V. Kharissova
Facultad de Ciencias Físico-Matemáticas, UANL, Monterrey, México
Pedro de Alba S/N, Ciudad Universitaria, C.P. 66450, San Nicolás de los Garza, N.L. México

S. Velumani, L. E. Garza Castañón
ITESM Campus Monterrey
Ave. Eugenio Garza Sada #2501 Sur Col. Tecnológico, Monterrey Nuevo León, México, C.P. 64849
(Recibido: 30 de noviembre de 2009; Aceptado: 23 de abril de 2010)

Results obtained by open circuit and potentiodynamic tests directly on a PEM fuel cell for a nanostructured $Pd_{70}Co_{20}Mo_{10}$ MEA are reported. A comparison of these results with the open circuit results obtained from a commercial Pt MEA is made, showing that although there´s lower efficiency of the trimetallic catalyst, it is feasible to develop new Platinum-free MEA´s. Background work involved ab-initio calculations using Materials Studio™ software to estimate catalyst structure and reaction capability to dissociate H_2 molecule, as well as the synthesis of a trimetallic catalyst at the nanometric level. Chemical composition for the nanostructured anodic and cathodic trimetallic catalyst is determined by AES and compared to the AES pattern obtained for the bulk $Pd_{70}Co_{20}Mo_{10}$.

Keywords: PEM fuel cell; Trimetallic catalyst; MEA; Potentiodynamic test; Auger spectra

1. Introduction

Fuel cells have been widely studied [1-10] in the last decades since they represent a clear path to producing electric energy. Of particular interest is the case of the proton exchange membrane (PEM) fuel cells because of their high-power densities and relatively low operation temperatures from 55 to 80 ^oC. Several approaches have been done to develop low-cost, high performance [11-19] PEM fuel cells membranes by improving the electrodes [20-23], modeling [24-26] and instrumentation techniques [27-30]. These approaches involve efforts to improve the membrane-electrodes assemblies (MEAs) [31-35], by developing composite catalysts to improve the CO-tolerance of the fuel cell, fuel reforming, etc. Although Pt is the major contributor to the cost of a fuel cell, it is still an object of research [36-39]. The purpose of this work is to show results obtained for a MEA prepared by depositing carbon support directly on the nafion™ membrane by electric arc technique, and deposit $Pd_{70}Co_{20}Mo_{10}$ trimetallic compound as anodic and cathodic catalysts synthesized at the nanoscale to increase the catalytic surface of the MEA. Background work involved the use of computer simulation techniques to develop an atomistic model (crystal lattice) for the trimetallic compound that solved for both the experimental XRD pattern and the chemical composition Pd:Co:Mo of 70:20:10 %. Also, synthesis of the catalyst at the nanostructure level is carried out to provide more surface area for the dissociation reaction (H_2) and reduction reaction (O_2). Final stage of this work is to test the MEA directly on a PEMFC, obtaining its open circuit and potentiodynamic behavior. Open circuit results are then compared with one obtained from a commercial Pt MEA.

2. Materials and methods

A 2.4 GHz, 200 GB PC was used for the calculations. The software was Materials Studio™ with its Reflex (XRD simulation) module.

a) Raw materials

For the synthesis of the nanostructured catalysts, a Pd-Co-Mo (70:20:10 %) target of size 50 mm diameter and 6.4 mm thickness was used. As proton exchange membrane, a 50X50 mm sized Nafion 112 ™ membrane was used (Dupont). 7-mm Graphite bar was used as the anode and cathode for the electric arc equipment to be deposited as the catalyst's support.

b) Equipment

For the carbon support deposition, a JEOL JEE-400 vacuum evaporator was used. To synthesize catalytic nanoparticles it used the inert gas condensation (ICG) technique and the equipment was a Nanosys 500 ultra-

* magarza@comimsa.com

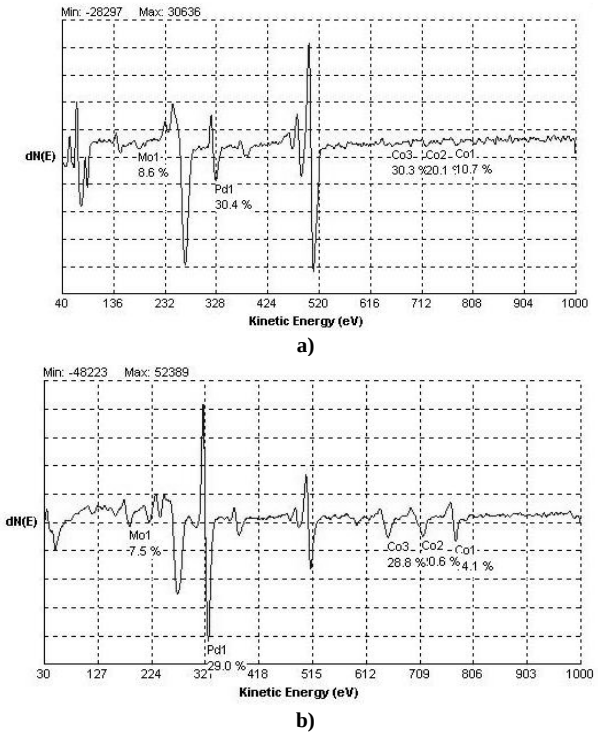

Figure 1. AES spectra for Pd-Co-Mo: (a) target, (b) 3-nm deposit.

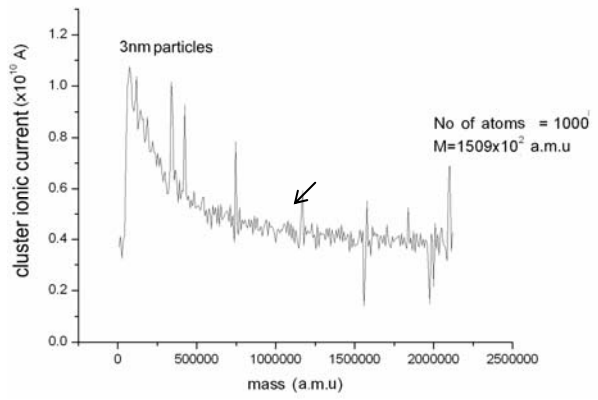

Figure 2. On-line measurement of the trimetallic nanoparticles.

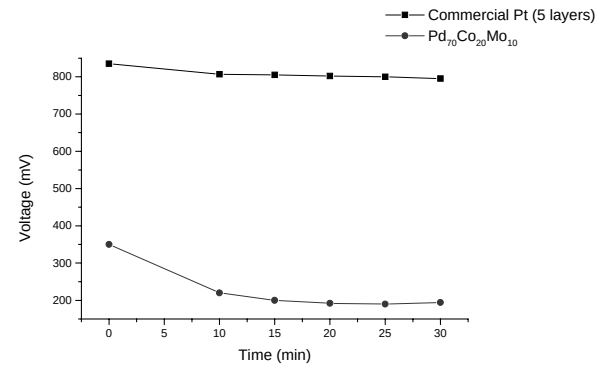

Figure 3. Open circuit test results for commercial Pt and Pd-Co-Mo nanostructured MEA (dry conditions).

high-vacuum system (Mantis ltd.). To characterize structure, a D-5000 (Siemens) X-ray difractometer was used. Particle size was on-line characterized within the IGC deposition system by a quadrupole mass filter. Elemental analysis was carried by Auger spectroscopy (AES) technique to compare between target's and nanoparticles deposit composition. Electrochemical characterization was carried out directly in a Solartron SI 1287 (1 pA sensitivity) coupled to a single PEM fuel cell, composed by a couple of bipolar plates with an active area of 22 mm x 25 mm and a gas diffusion layer of 28 mm x 28 mm.

3. Theoretical calculations

Using the materials studio software, an atomistic model, which will simulate the crystal lattice of the real compound accomplishing both the chemical composition and XRD pattern, was developed for the $Pd_{70}Co_{20}Mo_{10}$ compound. For comparison, experimental XRD pattern for Pd-Co-Mo is taken from the target, and Scherrer's formula was considered to calculate the lattice parameter and build up the atomistic model. To assure the correct description of the structure, a simulation of the XRD diffraction pattern was run using the Reflex module of Materials Studio ™ software. The simulated difractometer was set to X-Ray, Copper Kα source, with a wavelength of 1.54056 Å.

4. Experimental

XRD was taken for the target, in order to have a comparison with the nanoparticles produced and the atomistic model developed with the use of Materials Studio software. The Siemens D-5000 difractometer was set to a 35 KV potential, 25 mA current with a CuKα (λ = 1.5406 Å) anode and a W filament, with a Ni secondary monochromator. The step time was set to 1.1 sec, the step size used was 0.05°, scan angles were fixed from 2θ = 5° to 90°. Rotation was set to 15 RPM.

Graphite was deposited on the Nafion 112 membrane on both faces using the JEE-400 vacuum evaporator. Vacuum pressure was set to $4x10^{-3}$ Pa. Distance from electrodes to membrane was fixed to be 150 mm, since temperature rise during the electric arc generation may lead to burn the membrane. Deposition time was 25 seconds. Pd-Co-Mo 3-nm particles were deposited by IGC technique on the carbon-covered membrane. Ultra-high-vacuum pressure was set to 4.3 x 10^{-8} torr. Condensation zone was set to 92 mm, with an Ar and He flow of 10 and 20 sccm. Membranes were prepared by this method, with a deposition time of 75 minutes. After deposition of the electrodes, the MEA was subjected to a heat treatment at 85 °C during 30 minutes to obtain diffusion of the catalytic nanoparticles in the carbon substrate.

Open circuit and potentiodynamic (current production) tests were carried out using the Solartron SI 1287 equipment coupled to a single PEM fuel cell. Assembling torque was set to 2.8 N*m to avoid gas leaks. Work pressure was set to 1034.3 torr for the anode (hydrogen) as

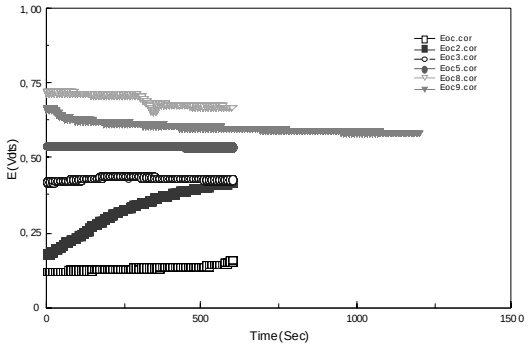

Figure 4. Open circuit test results for Pd-Co-Mo nanostructured MEA.

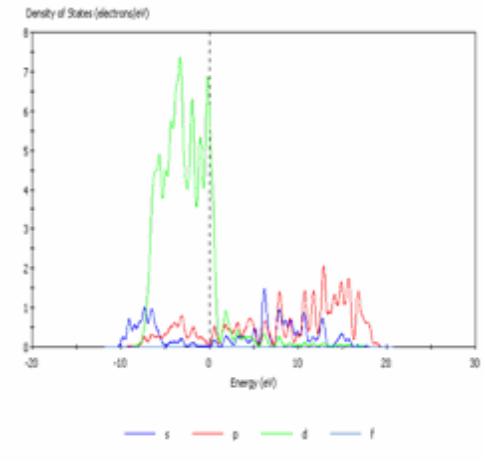

a)

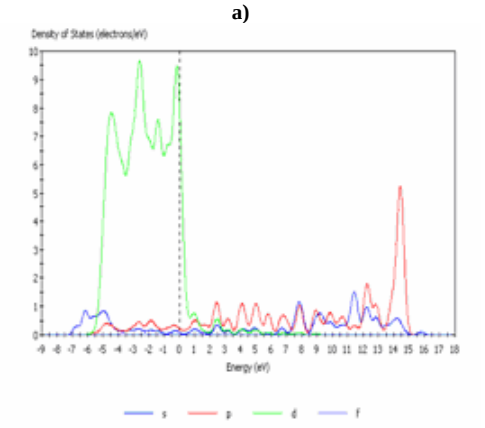

b)

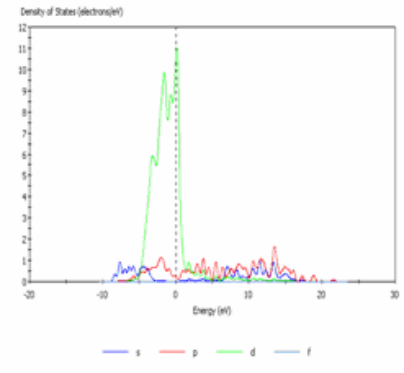

c)

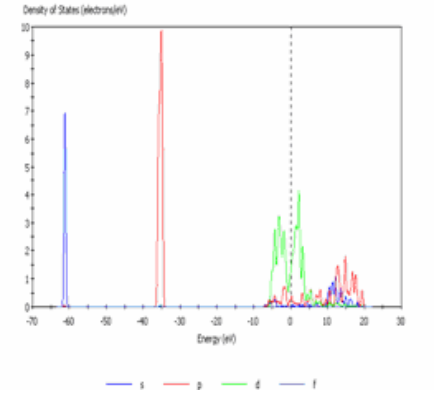

d)

Figure 5. Density of States (DOS) calculated for (a) Pt, (b) Pd, (c) Co and (d) Mo.

well as for the cathode (oxygen). Cell temperature was 40 ^{o}C. The gas feeding system allowed us to feed dry or humidified hydrogen to the anode. For the humidified hydrogen tests the humidifier temperature was set to 38 ^{o}C.

5. Results and discussion

An atomistic model was developed for Pd-Co-Mo compound that satisfied both structure (fcc-like) and chemical composition (70:20:10 %), the crystal was created from the experimental data reported by Raghuveer et al [35], and positions of the atoms were estimated to accomplish chemical composition and XRD pattern. Comparison between experimental and calculated XRD pattern was conducted to demonstrate that the experimental pattern taken from the sputtering target and simulated XRD pattern match in a highly reliable way. From the Scherrer´s equation (1.1) a crystallite size is estimated to be 48.2 nm, and simulated XRD pattern and structure are refined to fit the experimental data.

$$\Delta(2\theta)_{hkl} = \frac{180\,\lambda}{(\pi L_{hkl}\cos\theta)} \qquad (1.1)$$

where:

$\Delta(2\theta)_{hkl}$ = FWHM in the direction hkl
λ = X-ray wavelength (1.5406 Å)
L_{hkl} = crystallite size in the direction hkl
θ= diffraction angle

Nanoparticles were synthesized by the Nanosys 500. Auger spectroscopy was carried out on the 3-nm deposit and compared with that of the target. Results derived from AES (Fig.1) show a good correlation between elemental composition of the target and that of the nanostructured Pd-Co-Mo, which implies that no significant change occurred for the chemical composition of the compound.

Figure 2 shows the on-line measurement realized by the quadrupole mass filter inside the IGC deposition system. Highest peak correspond to 3 nm $Pd_{70}Co_{20}Mo_{10}$ particles.

Table 1. Reaction energies for H_2-metal (111) surface.

Metal	**Reaction energy** (eV)
Pt	-0.591
Pd-Co-Au	-0.531
Pd-Co-Mo	-0.396
Pd-Co-Ni	-0.238

Considering a spherical approach of the nanoparticle and a density of the trimetallic compound of 11.2 gr/cm^3, the diameter associated with the average mass of 1509x10^2 amu is calculated to be between 3.47 and 3.52 nm.

From results obtained under dry conditions (Fig.3) for both commercial Pt MEA and the proposed Pd-Co-Mo nanostructured MEA, it is clear that the capability of the trimetallic catalyst to dissociate the hydrogen molecule is lower than that of the commercial Pt. Lower amounts of carbon to provide more charge carriers and to develop efficient ionic channels for the conduction across the membrane may have resulted in a poor charge production for conduction. The absence of Pt on the electrodes as well as the lower volume of the carbon substrate decreases the hydrogen dissociation capability of the assembly, resulting in a poor OCV of the Pd-Co-Mo nanostructured MEA.

Results derived from the open circuit tests (Fig. 4) show the evolution in time of the open circuit voltage (OCV) of the assembly. The Eoc curve exhibits the open circuit voltage status when hydrogen and oxygen were dry-supplied (i.e. membrane wasn´t hydrated). Eoc2 shows the variation of the OCV along the hydration process through the feeding of hydrogen previously humidified. Eoc3 shows the variation of the OCV at a fixed humidification rate. It is well known that the humidification of the system will result in the membrane´s (electrolyte´s) ionic-conduction increasing, so, its contribution to the formation of redox pairs will be reflected in the growth of the OCV along the Eoc2 curve (from 130 mV up to 416 mV). Although Eoc5 curve shows higher OCV probably due to the extended period of humidification of the membrane, it becomes unstable and highly sensitive to variations in operating conditions as opening the system (oxygen flow) or closing the system (no flow for both hydrogen and oxygen) shows in Eoc8 and Eoc9 respectively.

The current production observed for the proposed MEA is about 3 μA/cm^2. Such current production is significantly lower (0.011 %) than that achieved by any commercial Pt assembly, which is about 26.7 mA/cm^2, according to [40].
Figure 5 shows a Density of States (DOS) calculation for Pt, Pd, Co, and Mo. According to the "d" band model for the reactivity of a metallic surface [41], the shift of the Platinum d-band center toward the Fermi energy explains its higher reactivity to hydrogen, but its highest reactivity makes platinum vulnerable to the attack of the contaminant specie (carbon monoxide) that covers active sites decreasing the ability to dissociate hydrogen. For the case of the combination Pd-Co-Mo, lowest occupancy of the "d" orbital represent less reactivity to hydrogen, but makes it more resistant to the attack of the CO specie, leaving active sites available for the hydrogen dissociation reaction.

The proposed technique to prepare the MEA has the advantage of using vacuum and ultra-high vacuum environment, which allowed us to obtain very low contamination for the prepared MEA. Cost comparison between that of a commercial Pt MEA ($ 104 usd) and the one developed using the proposed methodology ($ 4.63 usd), which represents 4.5 % of the cost of the commercial MEA yield to consider further investigation to improve current production of the proposed MEA. Although lower efficiency shown by the proposed MEA compared with the commercial Pt MEA, cost comparison can give us a glance of the economical benefit of developing Pt-free MEAs.

6. Conclusions

From computer calculations shown in Table 1, an estimation of the catalytic capability for a trimetallic compound might be carried out to save experimental time since its results can be used to make decisions before the synthesis of the catalytic particles. Results show that although Pt is the best catalyst for the hydrogen dissociation reaction, Pd-Co-Mo compound shows good catalytic properties too, with the compromise of lower catalytic activity.

Auger analysis (Fig. 1) showed good elemental-composition conservation while passing from the bulk material to the nanostructured Pd-Co-Mo, which was desired since computer calculations and estimates were based on the bulk's material structure and composition.

Density of states (DOS) analysis carried out for both Pt and the trimetallic catalyst shows the benefits of choosing a trimetallic alloy instead of the pure Pt catalyst, considering the lowest susceptibility of the trimetallic catalyst to the attack of poisoning specie as carbon monoxide, with the compromise of reducing the hydrogen dissociation capability of the MEA.

Under the assumption that the Pd-Co-Mo catalyst's structure was not inducing any limitation to the type of mass and charge-transport processes taking place inside the cell, and considering that the current production is an extensive property, the poor current density observed may be attributed to the small amount of catalytic material deposited on the electrodes. It must be considered that this fabrication process didn't include an ionic conductor in the electrodes that could have induced strong voltage drops in the system, as well as not providing ionic paths to complete the faradaic processes of the reaction. Thus, the electrodes fabrication process might be improved by the addition of an ionic conductor in order to increase the current production of the assembly.

On the basis of economy and cleanliness, further investigation must be considered for the enhancement of the current production of the proposed MEA given the potential savings that can be achieved migrating from a Pt-based technology to a Pt-free technology.

References

[1]. A. Bieberle, *The electrochemistry of Solid Oxide Fuel Cell Anodes: Experiments, modeling and simulations*, Doctoral and habilitation Theses (Swiss Federal Institute of Technology, Zurich, 2000).
[2]. K.D. Kreuer, Journal of membrane science, 185, 29 (2001).
[3]. B.C.H. Steele, A. Heinzel, Nature, 414, 345 (2001).
[4]. A. Bauen, D. Hart, Journal of power sources, **86**, 482 (2000).
[5]. G. Mackerron, Journal of power sources, **86**, 28 (2000).
[6]. G. Cacciola, V. Antonucci, S. Freni, Journal of power sources, **100**, 67 (2001).
[7]. J. Bockris, International journal of hydrogen energy, **27**, 731 (2002).
[8]. J.M. Ogden, M. Steinbugler, T. Kreutz, Journal of power sources, **79**, 143 (1999).
[9]. S. Ahmed, M. Krumpelt, International journal of hydrogen energy, 26, 291 (2001).
[10]. M.L. Perry, T.F. Fuller, Journal of the electrochemical society, **149**, S59 (2002).
[11]. M. Mathias, J. Roth, J. Fleming, W. Lehnert, *Chapter 46: diffusion media for PEM fuel cells*, Handbook of fuel cells-fundamentals, technology and applications, Vol. 3: fuel cells technology and applications, John Wiley and sons ltd. (New York, USA, 2003).
[12]. P. Costamagna, C. Yang, A.B. Bocarsly, S. Srinivasan, Electrochimica acta, **47**, 1023 (2002).
[13]. F.M. Vichi, M.T. Colomer, M.A. Anderson, Electrochemical and solid-state letters, 2 (7), 313 (1999).
[14]. W. Cui, J. Kerres, G. Eigenberger, Separation and purification technology, **14**, 145 (1998).
[15]. P. Genova-Dimitrova, B. Barallie, D. Foscallo, C. Poinsignon, J.Y. Sánchez, Journal of membrane science, **185**, 59 (2001).
[16]. S. Gamburzev, A.J. Appleby, Journal of power sources, **107**, 5 (2002).
[17]. N. Jia, M.C. Lefevre, J. Halfyard, Z. Qi, P.G. Pickup, Electrochemical and solid-state letters, **3**, 529 (2000).
[18]. J. Kerres, A. Ullrich, F. Meier, T. Haring, Solid state ionics, **125**, 243 (1999).
[19]. T. Okada, Journal of electroanalytical chemistry, **465**, 1 (1999).
[20]. Shin S.-J., Lee J.-K., Ha H.-Y., Hong S.-A., Chun H.-S., Oh I.-H., Journal of power sources, **106**, 146 (2002).
[21]. E.B. Easton, P.G. Pickup, Electrochemical and solid-state letters, **3**, 359 (2000).
[22]. E.B. Easton, Z. Qi, A. Kaufman, P.G. Pickup, Electrochemical and solid-state letters, **3**, A59 (2001).
[23]. X. Wang, I.-M. Hsing, Electrochimica acta, **47**, 2981 (2002).
[24]. G. Maggio, V. Recupero, L. Pino, Journal of power sources, **101**, 275 (2001).
[25]. L. Pisani, G. Murgia, M. Valentini, B. D'aguanno, Journal of the electrochemical society, **149** , A898 (2002).
[26]. J.S. Yi, T.V. Nguyen, Journal of the electrochemical society, **146**, 38 (1999).
[27]. B. Andreaus, A.J. McEvoy, G.G. Scherer, Electrochimica acta, **47**, 2223 (2002).
[28]. A.A. Kulikovsky, Electrochemistry communications, **4**, 527 (2002).
[29]. Baldauf M., Preidel W., Journal of applied electrochemistry, **31**, 781 (2001).
[30]. M.C. Lefevre, R.B. Martin, P.G. Pickup, Electrochemical and solid-state letters, **2**, 259 (2001).
[31]. M.S. Loffler, B. Gross, H. Natter, R. Hempelmann, T. Krajewski, J. Divisek, Physical chemistry & chemical physics, **3**, 333 (2001).
[32]. Y. Zhang, C. Erkey, Industrial and Engineering Chemistry Research, **44**, 5312 (2005).
[33]. N.P. Subramanian, S.P. Kumaraguru, H. Colon-Mercado, H. Kim, B.N. Popov, T. Black, D.A. Chen, Journal of Power Sources, **157**, 56 (2006).
[34]. H. Kim, B.N. Popov, Electrochemical and Solid-state Letters, **7**, A71 (2004).
[35]. V. Raghuveer, A. Manthiram, A.J. Bard, Journal of physical chemistry B, **109**, 22909 (2005).
[36]. U.B. Suryavanshi, C.H. Bhosale, Journal of Alloys and Compounds, **476**, 697 (2008).
[37]. C. Coutanceau, S. Brimaud, C. Lamy, J.-M. Léger, L. Dubau, S. Rousseau, F. Vigier, Electrochimica Acta, **53**, 6865 (2008)
[38]. B. Moreno, E. Chinarro, J.C. Pérez, J.R. Jurado, Applied Catalysis B: Environmental, **76**, 368 (2007).
[39]. X. Zhang, F. Zhang, R.-F. Guan, K.-Y. Chan, Materials Research Bulletin, **42**, 327 (2007).
[40]. http://www.fuelcellstore.com/en/pc/viewPrd.asp?idcategory=52&idproduct=1103, (2010).
[41]. A. Gross, Department of theoretical chemistry- university of Ulm, http:// www.uni-ulm.de/theochem, (2007).